Graded-index polymer optical fiber for high-speed data communication

Takaaki Ishigure, Eisuke Nihei, and Yasuhiro Koike

We successfully obtained a high-bandwidth (1 GHz km) and low-loss (90 dB/km at 0.572 μm of wavelength) graded-index polymer optical fiber by using the interfacial-gel polymerization technique, in which we used an unreactive component to obtain the quadratic refractive-index distribution. This high-bandwidth graded-index polymer optical fiber makes it possible to transmit a high-speed optical signal in a short-range network, which is not possible when we use the step-index type of polymer optical fiber commercially available.

Key words: Graded index, polymer optical fiber, interfacial-gel polymerization technique, high bandwidth, low loss.

Introduction

For long-range optical communication a single-mode glass optical fiber has been widely used, because of its high transparency and high bandwidth. In contrast, for short-range communication, recently there has been considerable interest[1,2] in the development of polymer optical fibers (POF's). In short-range communications (such as local area network systems, interconnections, the termination area of fiber to the home, and domestic passive optical network concepts[3]), many junctions and connections of two optical fibers would be necessary. In a single-mode fiber the core diameter is approximately 5–10 μm, so when one connects two fibers, a slight amount of displacement such as a few micrometers causes a significant coupling loss. The POF is one of the promising possible solutions to this problem, because commercially available POF usually has a large diameter such as 1 mm. Therefore, low transmission loss and high bandwidth has been required for POF's to be used as a short-distance communication media.

All commercially available POF's, however, have been of the step-index (SI) type. Therefore, even in short-range optical communication, the SI POF will not be able to cover the whole bandwidth of the order of hundreds of megahertz that will be necessary in fast datalink or local area network systems in the near future, because the bandwidth of the SI POF is only approximately 5 MHz km.

In contrast, graded-index (GI) POF is expected to have a much higher bandwidth than SI POF, while maintaining a large diameter. We have proposed some preparation techniques of GI POF that use copolymerization.[4–7] Here we obtain a low-loss and high-bandwidth GI POF with good flexibility by using a different technique. The formation of the GI and the optical properties of such a GI POF are described here.

Preparation of Graded-Index

Materials

The preform with a 10-mm diameter, in which the refractive index gradually decreases from the center axis to the periphery, was prepared by an interfacial-gel polymerization technique. In the previous interfacial-gel copolymerization technique,[6,7] two monomers, M_1 and M_2, with different refractive indices and reactivities were copolymerized. For example, methyl methacrylate (MMA) and vinyl benzoate (VB) were selected as M_1 and M_2 monomers, respectively. In the interfacial-gel polymerization technique, we select the M_1 monomer with a low refractive index as well as an unreactive component with a high refractive index (instead of the M_2 monomer) to form the GI preform. Here we select MMA and bromobenzene (BB) as the M_1 monomer and the unreactive component, respectively, whose properties are shown in Table 1.

The monomer MMA (Wako Chemical Company)

The authors are with the Faculty of Science and Technology, Keio University, 3-14-1, Hiyoshi, Kohoku-ku, Yokohama 223, Japan.

Received 15 June 1993; revised manuscript received 19 October 1993.

0003-6935/94/194261-06$06.00/0.

Table 1. Properties of the Used Monomer, Homopolymer, and Unreactive Component

Parameter	MMA	PMMA	BB
Molecular weight	100.1		1.57
Density	0.94	1.19	1.5
Refractive index	1.42	1.49	1.56

was purified as follows: we removed the inhibitors from the monomer by rinsing with a 0.5N NaOH aqueous solution, and we then washed out the remaining NaOH with distilled water several times. The monomer was dried with calcium hydride, filtered through a membrane filter whose pore size was 0.2 μm, and distilled with reduced pressure.

BB (also from Wako Chemical Co.) was used without further purification. 1,1-bis(*t*-butylperoxy)3,5,5-trimethylcyclohexane (from Nippon Oil and Fats Co.) was used as an initiator and *n*-butylmercaptan (from Wako Chemical Co.) was used as a chain transfer agent, both without further purification.

Formation of Graded Index

As we stated above, we used BB, instead of the M_2 monomer, as the unreactive component with a high refractive index. MMA and BB monomer mixtures with specified amounts of 1,1-bis(*t*-butylperoxy)3,5,5-trimethylcyclohexane and *n*-butylmercaptan were placed in a poly(methyl methacrylate) (PMMA) tube prepared in our laboratory, the outer and inner diameters of the tube were 10 and 6 mm, respectively. The PMMA tube filled with the monomer mixture was placed in a furnace at 90–95 °C for 24 h.

First the inner wall of the PMMA tube swells slightly toward to the monomer mixture; then a gel phase is formed on the inner wall of the tube. This state is shown schematically in Fig. 1(A). Here, because the rate of the polymerization reaction inside the gel is much faster than that in the monomer liquid phase because of the gel effect, the polymerization occurs from the inner wall of the tube.

As the polymer phase thickened, the concentration of the M_2 molecules in the monomer liquid phase gradually increased at the center region of the tube because of the dissolution of the PMMA homopolymer into the monomer liquid phase from the tube and because of the gradual diffusion of the MMA molecules and BB molecules into the gel phase. Here, because the molecular volume of BB is slightly larger than that of MMA, MMA molecules can more easily diffuse into the gel phase than BB molecules. Therefore, the concentration of BB in MMA monomer at the center region increased. Also note that the polymer phase gradually thickened, while the polymer content of the monomer liquid phase at the center region slightly increased. This is shown schematically in Fig. 1(B).

Next, as shown in Fig. 1(C), the polymer phase reached the center axis of the PMMA tube and the GI preform rod was obtained. We heat treated the GI preform at 110 °C under 0.2 Torr for 24 h to complete the polymerization. We obtained the GI optical fiber by heat drawing the preform at 160–190 °C. We obtained a GI POF with the desired diameter by controlling the velocity at which the fiber is taken up. The diameter of the GI POF was controlled to 0.5 mm in this experiment.

Results and Discussion

Characteristics of the Graded-Index Preform

Refractive-Index Distribution

We measured the refractive index distribution of the preform by using the longitudinal interferometric technique,[8] shown as curves (A), (B), and (C) of Fig. 2, in which n_0 and n are the refractive indices at the center axis and at distance r from the center axis, respectively, and in which R_p is the radius of the preform. All the preform rods have cladding corresponding to the PMMA tube and have an almost quadratic index profile at the core region. The refractive-index difference between n_0 and n_c (refractive index of cladding) decreases with an increase in the ratio of BB to MMA (MMA/BB, wt/wt), because the

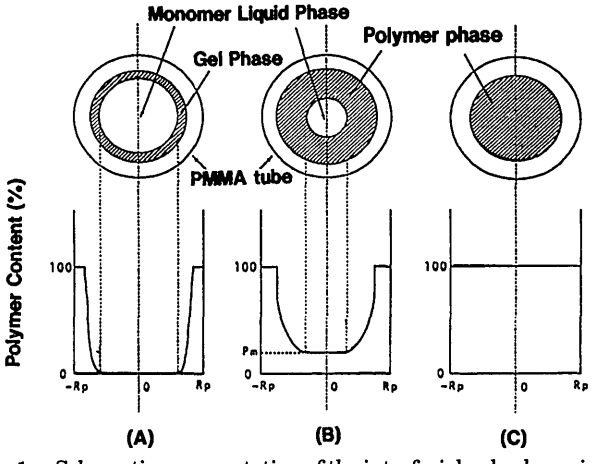

Fig. 1. Schematic representation of the interfacial-gel polymerization technique.

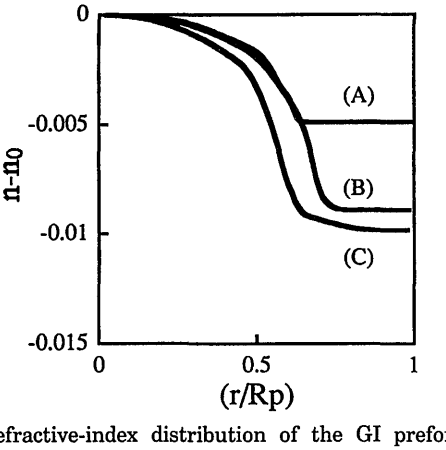

Fig. 2. Refractive-index distribution of the GI preform: (A) MMA/BB = 10/1, (B) MMA/BB = 7/1, (C) MMA/BB = 5/1.

BB concentration at the core center becomes higher as the ratio of BB to MMA increases.

Light-Scattering Loss

It is well known that the attenuation of optical transmission through fiber is caused by absorption and scattering. To measure the light-scattering loss and investigate the heterogeneities inside the preform rod we measured polarized (Vv) and depolarized (Hv) light-scattering intensities from a He–Ne laser (0.633-μm wavelength) against the scattering angle, θ. Although the Hv intensity was independent of scattering angle and was approximately 10^{-6}–10^{-7} cm^{-1}, the Vv intensity strongly increased with a decrease of the scattering-angle forward scattering in the range of 10^{-5}–10^{-6} cm^{-1}. In randomly oriented polymer bulks, the isotropic part, Vv^{iso}, of Vv is given by[8]

$$Vv^{iso} = Vv - (4/3)Hv. \quad (1)$$

Therefore, the observed Vv scattering was divided into three therms, Vv_1^{iso}, Vv_2^{iso}, and $(4/3)Hv$, as follows:

$$Vv = (Vv_1^{iso} + Vv_2^{iso}) + (4/3)Hv, \quad (2)$$

where Vv_1^{iso} denotes the isotropic background scattering independent of the scattering angle, and Vv_2^{iso} is the isotropic scattering that depends on the scattering angle caused by large-size heterogeneities. Finally, the total scattering loss α_t (decibels per kilometer) is obtained by

$$\alpha_t = 1.346 \times 10^6 \int_0^{\pi} \left[(1 + \cos^2\theta)(Vv_1^{iso} + Vv_2^{iso}) + (13 + \cos^2\theta)\frac{H_v}{3} \right] \sin\theta d\theta. \quad (3)$$

Here α_t is divided into three terms, α_1^{iso}, α_2^{iso}, and α^{aniso}. That is,

$$\alpha_t = \alpha_1^{iso} + \alpha_2^{iso} + \alpha^{aniso}. \quad (4)$$

To investigate the heterogeneous structure by using the angular dependence of the Vv_2^{iso}, we used Debye's fluctuation theory,[9] in which the correlation function $\gamma(r)$ was approximated by $\exp(-r/a)$. Here, the heterogeneous structure with the mean-square average of the fluctuation of all dielectric constants is described by $\langle\eta^2\rangle$. Details of these estimation methods from the Vv_2^{iso} are described elsewhere.[5]

Table 2 shows the results of these scattering data for the GI preform rods, compared with those of the MMA–VB GI preform rod previously reported.[10] It is confirmed that the Vv_2^{iso} is caused by the heterogeneities with dimensions of 500–1200 Å of the order of $\langle\eta^2\rangle = 10^{-8}$. It is noteworthy that the total scattering losses α_t for the GI preform rods of MMA/BB = 5.0 (wt/wt) are only approximately 30 dB/km and are comparable with those of PMMA homopolymer.[11] In the case of the MMA–VB system preform, the isotropic scattering loss with angular interdependence (α_1^{iso}) is almost the same as that of the MMA–BB system preform, whereas the isotropic scattering loss with angular dependence (α_2^{iso}) is twice as high.

Table 2. Scattering Parameters of MMA-BB and MMA–VB GI POF's at 0.633 μm

Ratio	a (Å)	$\langle\eta^2\rangle$ ($\times 10^{-8}$)	α_1^{iso} (dB/km)	α_2^{iso} (dB/km)	α^{aniso} (dB/km)	α_t (dB/km)
MMA/BB						
5/1	722	0.45	8.2	19.1	7.3	34.6
7/1	774	0.16	19.6	7.5	4.3	31.4
MMA/VB						
5/1	762	0.74	6.1	33.9	10.1	50.1

Because these heterogeneities originate inside the copolymer glasses, we should also investigate the effect of the distribution of the copolymer composition. In the MMA–VB preform, we were able to calculate the distribution of the copolymer composition from the monomer reactivity ratio, details of which are described elsewhere.[12] The calculated result is shown in Fig. 3, in which the ratio of BB to MMA of MMA–VB is 4/1 (wt/wt). Figure 3 indicates that the distribution of the poly(MMA-co-VB) composition, where co stands for copolymer, is divided into main two components: one is the copolymer formed in the initial stage of polymerization and whose composition is quite similar to PMMA, and the other is the copolymer that is formed in the final stage of polymerization and is almost a VB homopolymer. From this result we see that the copolymer is virtually similar to a polymer blend of MMA and VB homopolymer. Assuming that the heterogeneities of these preform rods consist of two phases with volume fraction ϕ_1 corresponding to PMMA and volume fraction ϕ_2 corresponding to poly(vinyl benzoate), and with refractive indices n_1 and n_2, respec-

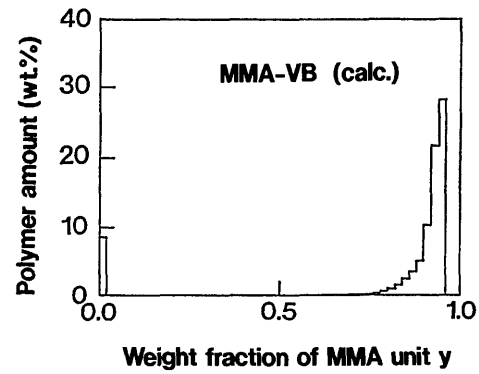

Fig. 3. Distribution of copolymer composition after 100% polymerization when MMA/VB = 4/1 (wt/wt).

tively, we see that $\langle \eta^2 \rangle$ is given by

$$\langle \eta^2 \rangle \cong \phi_1 \phi_2 (n_1 - n_2)^2, \quad (5)$$

$$\cong 4\phi_1 \phi_2 n^2 (\Delta n),$$

$$a = \frac{4V}{S} \phi_1 \phi_2, \quad (6)$$

where S is the total surface area of the boundary between the two phases, V is the total volume, n is the average refractive index, Δn is $(n_1 - n_2)$, and $\phi_1 + \phi_2 = 1$. From Eq. (5), we find that if $\phi_1 = 0.1$–0.9, the fluctuation of the refractive index is of the order of 10^{-5}.

In contrast, in the case of the MMA–BB system preform, PMMA and BB molecules are not phase separated but completely miscible. In Table 2 the experimental results of the light-scattering measurement of the MMA–BB system GI preform are shown. It should be noted that the isotropic scattering loss of the MMA–BB preform becomes lower than that of the MMA–VB preform. Therefore, it is considered that the BB molecules are not aggregated but randomly located and that there are no heterogeneous structures large enough in the MMA–BB preform to cause a high scattering loss.

Optical Properties of Graded-Index Polymer Optical Fiber

Refractive-Index Distribution

We measured the refractive-index distribution of the GI POF by using the transverse interferometric technique.[8] The refractive-index distribution of the MMA/BB = 5 (wt/wt) fiber is shown as curve F5 of Fig. 4 compared with that of the preform rod, curve P5, where n_0 and n are the refractive indices at the center axis and at distance r from the center axis, respectively. The index distribution of the fiber is almost quadratic against the normalized radius (r/Rp) and is almost the same as that of the preform rod. The numerical aperture estimated from the index difference is approximately 0.21.

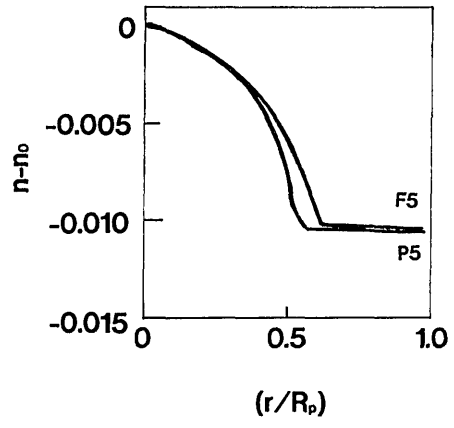

Fig. 4. Refractive-index distribution of the MMA–BB GI preform and the GI POF: P5, preform rod (10 mm ϕ); F5, fiber (0.5 mm ϕ).

Attenuation of Light Transmission

We measured the total attenuation spectrum of the light transmission through the GI optical fiber by using a spectrum analyzer (Advantest Model TQ8345). The result for the MMA/BB = 5(wt/wt) fiber is shown in Fig. 5. The minimum total attenuation was 90 dB/km at 0.572 μm of wavelength for the MMA/BB = 5 fiber. It should be noted that the attenuation of this MMA–BB system fiber is almost the same or is superior to that of SI POF's commercially available (100–300 dB/km). The dramatic decrease of the attenuation compared with our previous results[5–7] concerning MMA–VB (134 dB/km at a 0.652-μm wavelength) and MMA-vinyl phenylacetate (143 dB/km at a 0.651-μm wavelength) copolymer GI POF is attributed to the reduction of the scattering loss described above. It is noteworthy that the optical window of the MMA–BB GI POF is located near 0.57 μm of wavelength, whereas the optical window of the copolymer system GI POF such as MMA-co-VB or MMA-co-VPAc was located near 0.65 μm of wavelength.

Bandwidth

We measured the bandwidth of the GI and SI POF's by determining the impulse response function of the fiber. The experimental setup of this measurement system is shown in Fig. 6. A pulse of 10 MHz from an InGaAlP laser diode (wavelength, 0.67 μm) was injected (N.A., 0.5) into a 55-m-long fiber. We detected the output pulse with a sampling head (Hamamatsu Photonics Model OOS-01). The result for the MMA–BB GI POF, compared with that of the SI POF, is shown in Fig. 7. It is quite noteworthy that, although the output pulse through the SI POF is spread quite widely, the pulse through the GI POF is almost the same as the input pulse even after a 55-m signal transmission. The bandwidth of the SI POF estimated at the 3-dB level in the impulse response function is 5 MHz km, whereas the bandwidth of the MMA–BB GI POF in Fig. 7 is 1.0 GHz km, which is 200 times larger than that of the SI POF.

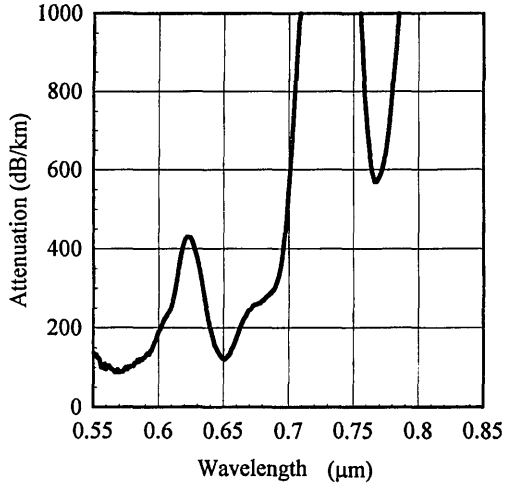

Fig. 5. Total attenuation spectrum of the GI POF.

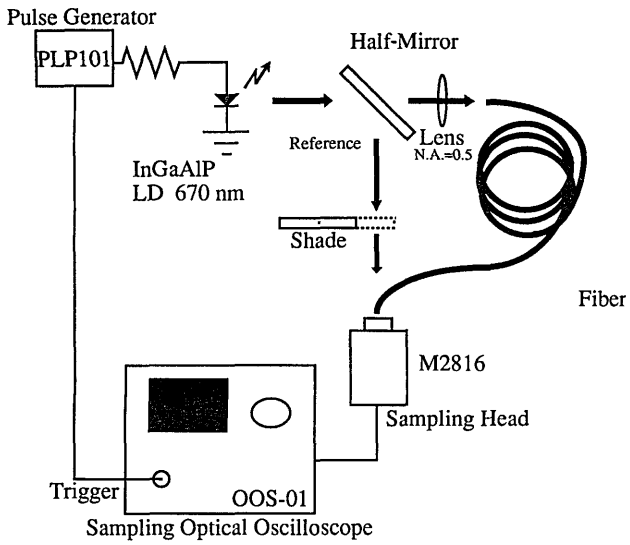

Fig. 6. Experimental setup of the impulse response function measurement; LD, laser diode.

It is well known that one can maximize the bandwidth by optimizing the shape of the refractive-index distribution of the fiber core. When the index distribution is expressed by a power law of the form

$$n(r) = n_0[1 - (r/Rp)^g\Delta], \tag{7}$$

the bandwidth is maximized for

$$g = 2 - (12/5)\Delta. \tag{8}$$

In this formula Δ is a parameter that measures the relative index difference, $\Delta = (n_0 - n_c)/n_0$, where n_0 and n_c are the index values at the core center and in the fiber cladding, respectively, and R_p is the radius of the core. The parameter g is the exponent of the power law. Because $\Delta = 0.01$–0.02 for the GI POF, the maximum bandwidth is achieved when g is approximately 2. The refractive-index distribution of this high-bandwidth GI POF is shown by the solid curve in Fig. 8. The index profile approximated by Eq. (7) through the use of a least-squares technique is shown by the dashed curve in Fig. 8. Figure 9 summarizes the bandwidth of the various GI POF's against the g in Eq. (7), along with that of the SI POF. The bandwidth is maximized near $g = 2$ for the MMA-BB fiber and is 1 GHZ km, which is 200 times larger than that of the SI POF.

The high bandwidth of the GI POF compared with that of the conventional SI POF was experimentally confirmed, even for a short-distance communication as small as 50 m. We measured the tensile strength of the GI POF by elongating a 100-mm length of POF

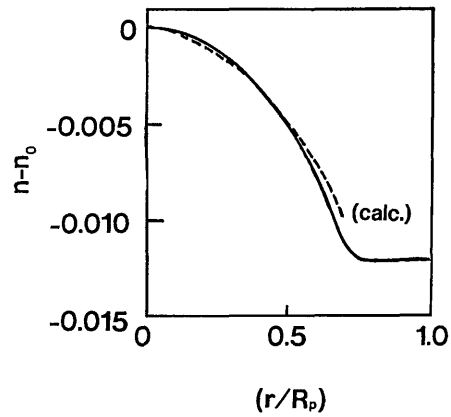

Fig. 8. Refractive-index distribution of the MMA–BB GI POF (solid curve) in which the bandwidth is 1 GHz km and the index profile (dashed curve) is approximated by Eq. (7).

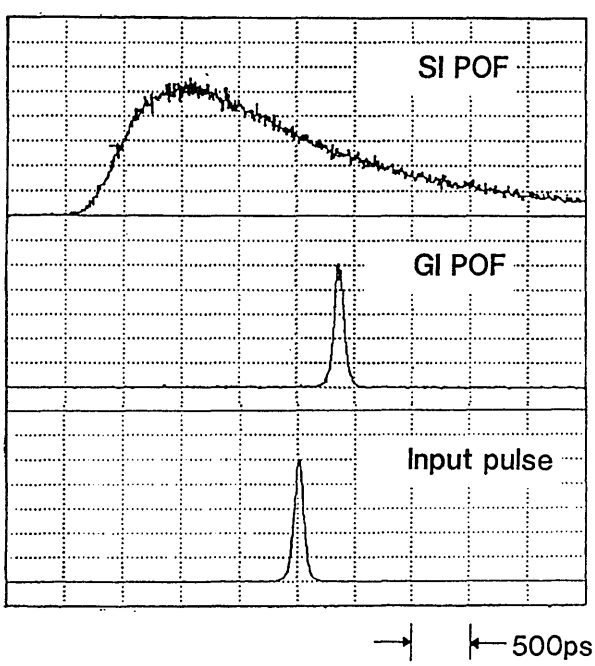

Fig. 7. Output pulse spread through both GI and SI POF's.

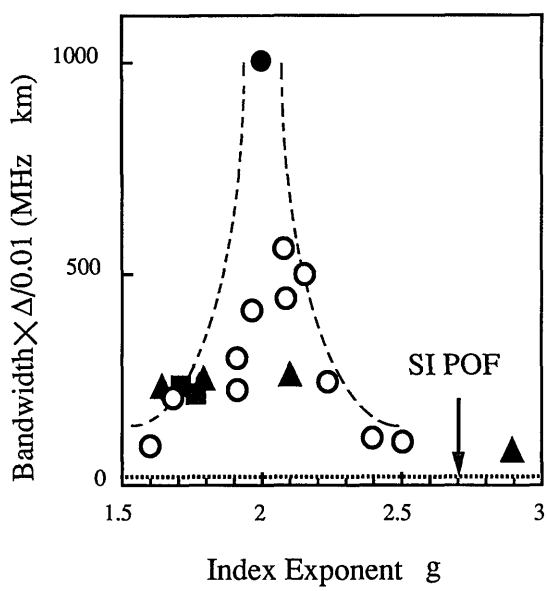

Fig. 9. Normalized bandwidth of GI POF's against index exponent g: ○, MMA–benzyl methacrylate system; ▲, MMA–VB system; ■, MMA–VPAc system; ●, MMA–BB System.

at a rate of 100 mm/min. The strength of the MMA–BB GI POF is 2000 kgf/cm^2, which is comparable with that of commercially available SI POF (900–1200 kgf/cm^2).

Conclusion

We successfully obtained a low-loss and high-bandwidth GI POF with good mechanical properties by utilizing the swelling of the polymer and the diffusion of the monomer molecules. This GI POF essentially consists of PMMA homopolymer, so the scattering loss is lower than that of the copolymer GI POF we previously prepared. Furthermore, as the refractive index of this GI POF monotonically decreases from the center axis to the periphery without any fluctuation, the bandwidth becomes three times higher than that of our previous MMA–VB copolymer GI POF.

References

1. C. Emslie, "Review of polymer optical fibres," J. Mater. Sci. **23,** 2281–2293 (1988).
2. W. Groh, D. Lupo, and H. Sixl, "Polymer optical fibers and nonlinear optical device principles," Angew. Chem. Int. Ed. Engl. Adv. Mater. **28,** 1548–1559 (1989).
3. G. D. Khoe and A. H. Dieleman, "TTOSS: Integrated subscriber system for direct and coherent detection," J. Lightwave Technol. **LT-4,** 778–784 (1986).
4. Y. Ohtsuka and Y. Koike, "Studies on the light-focusing plastic rod. 18: Control of refractive-index distribution of plastic radial gradient index by photocopolymerization," Appl. Opt. **24,** 4316–4320 (1985).
5. Y. Koike and Y. Ohtsuka, "Low-loss GI plastic fiber and novel optical polymers," Mater. Res. Soc. Symp. Proc. **172,** 247–252 (1990).
6. Y. Ohtsuka, E. Nihei, and Y. Koike, "Graded-index optical fibers methyl methacrylate-vinyl benzoate copolymer with low loss and high bandwidth," Appl. Phys. Lett. **57,** 120–122 (1990).
7. Y. Koike, E. Nihei, N. Tanio, and Y. Ohtsuka, "Graded-index plastic optical fiber composed of methyl methacrylate and vinyl phenylacetate copolymer," Appl. Opt. **29,** 2686–2691 (1990).
8. Y. Koike, N. Tanio, and Y. Ohtsuka, "Light scattering and heterogeneities in low-loss poly(methyl methacrylate) glasses," Macromolecules **22,** 1367–1373 (1989).
9. Y. Ohtsuka and Y. Koike, "Determination of the refractive-index profile of light-focusing rods: accuracy of a method using interphako interference microscopy," Appl. Opt. **19,** 2866–2872 (1980).
10. P. Debye, H. R. Anderson, and H. Brumberger, "Scattering by an inhomogeneous solid. II. The correlation function and its application," J. Appl. Phys. **28,** 679–683 (1957).
11. Y. Koike, S. Matsuoka, and H. E. Bair, "Origin of excess light scattering in poly(methyl methacrylate) glasses," Macromolecules **25,** 4809–4815 (1992).
12. Y. Koike, "High-bandwidth graded-index polymer optical fibre," Polymer **32,** 1737–1745 (1991).